Generalized relativistic meson wave function

Adam Szczepaniak, Chueng-Ryong Ji, and Stephen R. Cotanch
Department of Physics, North Carolina State University, Raleigh, North Carolina 27695-8202
(Received 11 June 1993)

We study the most general, relativistic, constituent $q\bar{q}$ meson wave function within a new covariant framework. We find that by including a tensor wave function component, a pure valence quark model is now capable of reproducing not only all static pion data (f_π, $\langle r_\pi^2 \rangle$) but also the distribution amplitude, form factor [$F_\pi(Q^2)$], and structure functions. Further, our generalized spin wave function provides a much better detailed description of meson properties than models using a simple relativistic extension of the $S = L = 0$ nonrelativistic wave function.

PACS number(s): 12.39.Ki, 13.60.−r, 14.40.Aq

I. INTRODUCTION

Since an exact solution to a bound-state problem in QCD is still unavailable many approximate treatments have been developed. Among them, the constituent quark model has perhaps received the most attention and is widely regarded as a very efficient and effective tool in description of hadronic phenomena [1–3]. The complex low energy structure of QCD currently precludes an unambiguous identification of the complete degrees of freedom and it is therefore important to continue to advance, refine and test the valence quark dominance approximation. Prospects are encouraging because new, precision data provided by future CEBAF experiments will significantly clarify this situation and also detail the role of exotic quark and/or gluon configurations. However, before the relative importance of valence versus exotic configurations can be established, uncertainties in the description of hadronic amplitudes due to valence quark model approximations must be reduced. In a previous study [4] we investigated alternative model approaches by comparing different relativistic formulations for the light pseudoscalar mesons. In particular, we developed and examined a covariant variable front approach which permitted quantitatively assessing the relevance of Lorentz covariance for any constituent formulation. We also established that pion and the kaon static properties can be well described by relativistic models utilizing constituent $q\bar{q}$ meson wave functions represented by the product of a noninteracting spinor component and a momentum space orbital amplitude. It is believed that such models will be able to describe low energy mesonic data to within 10–20 %. Unfortunately, there is still a large energy gap between this region and the energy-momentum scale where asymptotic freedom dominates [5] and a clear need exists for an improved, QCD related quark model to describe this intermediated regime. This is especially true for analyzing electromagnetic form factors with $Q^2 > 2 - 3$ GeV^2 for which all quark models described in Ref. [4] fail to describe the data. As mentioned above, however, before making any exotic extensions of the quark model an improved framework for the $q\bar{q}$ system must be developed. The purpose of this paper is to report one such attempt which utilizes a more general quark meson wave functions.

In this paper we extend our covariant variable front quark model by incorporating a more general spinor wave function with tensor components. Although not an observable, the wave function is constrained by results from QCD studies of moments of the distribution amplitudes [6–9]. Additional information comes from meson structure functions measured in Drell-Yan experiments [10–12]. In the next section we briefly review the basic assumptions of the covariant quark model, and detail our extended valence meson wave function. In Sec. III we analyze the quark distribution amplitudes and structure functions for the low lying mesons and present numerical results. Finally, we discuss and summarize our major results in Sec. IV.

II. VALENCE QUARK MESON WAVE FUNCTION

Following our previous paper we specify the quantization surface Σ by a timelike four vector n^μ with $n^2 = 1$, although the analysis is also appropriate for the case when n^μ is null-like, $n^2 = 0$ [13]. The transverse and longitudinal components of an arbitrary four-vector A^μ are denoted as A_T and A_L, respectively, $A^\mu = (A_L, A_T)$ and are defined by

$$A_L \equiv n \cdot A, \quad A_T^\mu \equiv A^\mu - A_L n^\mu.$$

Since $n \cdot A_T = 0$, A_T^μ has only three independent components which we label $(A_T^\perp, A_T^3)$ and henceforth identify by A_T. We define the wave function $\Psi^\alpha(k_{Ti}; \lambda_i; \tau_i), i = 1, \ldots, N$ as the probability amplitude for finding N constituents (quarks, antiquarks, gluons) with transverse momenta k_{Ti}, helicities λ_i, and flavor-color components τ_i in a meson state α ($\alpha = 1, \ldots, 8$ for the pseudoscalar octet) with momentum $P_T = \sum_i k_{Ti}, P_L = \sqrt{M^2 + |P_T^2|}$ by the matrix element

$$\langle k_{Ti};\lambda_i;\tau_i|P_T;\alpha\rangle = (2\pi)^3\sqrt{2P_L}\delta^3(P_T-\sum_i k_{Ti})\left[\prod_i\sqrt{\frac{k_{iL}}{m_i}}\right]\Psi^\alpha(k_{Ti};\lambda_i;\tau_i). \tag{2.1}$$

Here the single particle states $|k_T;\lambda;\tau\rangle$ describe effective, massive constituents quantized on the spacelike surface Σ perpendicular to n^μ and the longitudinal momenta are constrained by the on shell condition

$$k_{iL} = \sqrt{m_i^2+|k_{iT}^2|}. \tag{2.2}$$

The single particle states are normalized according to

$$\langle k_T',\lambda',\tau'|k_T,\lambda,\tau\rangle = \frac{k_L}{m}(2\pi)^3\delta^3(k_T'-k_T)\delta_{\lambda'\lambda}\delta_{\tau'\tau} \tag{2.3}$$

for fermions and

$$\langle P_T',\alpha|P_T,\beta\rangle = 2(2\pi)^3P_L\delta^3(P_T'-P_T)\delta_{\alpha\beta} \tag{2.4}$$

for bosons.

The set of wave functions defined by Eq. (2.1) constitutes a Lorentz group representation basis. In a formalism with a fixed quantization surface, Lorentz transformations depending on interactions do not leave Σ invariant. Interactions do not conserve particle number and therefore as the system evolves different Fock sectors mix [14]. This in general leads to complicated transformation properties for the wave functions under the action of interaction-dependent generators of the Lorentz group. A simplification is usually made by using an interaction free transformation rule for the wave function in a given Fock sector [15]. The valence $q\bar{q}$ wave functions describing a meson state with four-momenta P and $P'=\Lambda P\equiv\mathcal{L}(P\to\Lambda P)P$, respectively, are thus related by

$$\frac{1}{\sqrt{2P_L}}\left[\prod_i\sqrt{\frac{k_{iL}}{m_i}}\right]\Psi^\alpha(k_{Ti};\lambda_i;\tau_i) = \prod_i\sum_{\lambda_i'}D_{\lambda_i\lambda_i'}(R_W)\frac{1}{\sqrt{2P_L'}}\left[\prod_i\sqrt{\frac{k_{iL}'}{m_i}}\right]\Psi^\alpha(k_{Ti}';\lambda_i';\tau_i) \tag{2.5}$$

with $k_i'=\Lambda k_i$ and $D_{\lambda\lambda'}(R_W)$ denoting the matrix representations of the Wigner rotation R_W in the spin space expressed in terms of $q\bar{q}$ momentum variables,

$$R_W = R_W(k_{iT}) = \mathcal{L}(\Lambda P\to\hat{P})\mathcal{L}(P\to\Lambda P)\mathcal{L}(\hat{P}\to P),$$

and $\hat{P}=(M,\mathbf{0})$ being the meson rest frame momentum. Using this approximation the meson state is defined in a standard way and contains only $q\bar{q}$ valence component. Equations (2.1) and (2.3) then lead to the wave function normalization:

$$\sum_{\lambda,\tau}\int[dk_{iT}]_P^{q\bar{q}}\Psi^{\dagger\alpha}(k_{iT};\lambda;\tau)\Psi^\beta(k_{iT};\lambda;\tau) = \delta^{\alpha\beta}, \tag{2.6}$$

$$[dk_{iT}]_P^{q\bar{q}} = [dk_{iT}]_P \equiv \prod_i^2\frac{d^3k_{iT}}{(2\pi)^3}(2\pi)^3\delta^3\Big(P_T-\sum_i^2 k_{iT}\Big).$$

In general, approximations and specifically Fock space truncations destroy covariance. Here the truncation generates noncovariance by the emergence of an unphysical dependence of matrix elements upon n^μ. In [4] we describe a method for restoring covariance by allowing the quantization surface Σ, or equivalently the quantization vector n^μ, to transform actively under Lorentz transformations by relating n^μ to the meson external momenta.

The normalization equation (2.6) is identical to the corresponding nonrelativistic expression in the meson rest frame, since the relativistic wave function is constructed to reduce to the nonrelativistic one in this frame. For the ground-state pseudoscalar octet the form of the relativistic wave function is then derived from Eq. (2.5) to be

$$\begin{aligned}\Psi^\alpha(k_{Ti};\lambda_i;\tau_i) &= \chi^\alpha_{\tau_1\tau_2}\xi(k_{iT};\lambda_i)\Phi(\mathcal{M}^2),\\ \chi^\alpha_{\tau_1\tau_2} &\equiv i\left[\frac{\lambda^\alpha}{\sqrt{2}}\otimes\frac{I}{\sqrt{3}}\right],\\ \xi(k_{iT};\lambda_i) &\equiv \sqrt{2}\frac{\sqrt{m_1m_2}}{\sqrt{\mathcal{M}^2-(m_1-m_2)^2}}\\ &\quad\times\bar{u}(k_{1T};\lambda_1)\gamma_5 v(k_{2T};\lambda_2),\end{aligned} \tag{2.7}$$

where λ^α are the Gell-Mann SU(3) flavor matrices, I is the identity matrix in the color space, m_1,m_2 are the quark and antiquark constituent masses, respectively, $\mathcal{M}$ is the $q\bar{q}$ invariant mass,

$$\begin{aligned}\mathcal{M}(k_i)\equiv(k_1+k_2)^2 &= [k_{1L}(k_{1T})+k_{2L}(k_{2T})]^2\\ &\quad+(k_{1T}+k_{2T})^2,\end{aligned} \tag{2.8}$$

with $k_{iL}(k_T)$ given by Eq. (2.2) and the spin-independent orbital wave function $\Phi(\mathcal{M})$ usually assumed by Gaussian,

$$\Phi(\mathcal{M}) = N\exp\left[-\frac{\mathcal{M}^2}{8\beta^2}\right]. \tag{2.9}$$

The overall normalization constant N is determined from Eq. (2.6).

As explained above the explicit form of the transverse variables will depend on the choice for n^μ which in turn will be specified after selecting which matrix element is to be calculated with the wave function of Eq. (2.7). The wave function specified by Eq. (2.7) has also been exten-

sively studied in [4] for fixed quantization schemes. Here we study the extension of Eq. (2.7) to the most general Dirac structure for the $q\bar{q}$ system. We write the spinor component $\xi(k_{iT};\lambda_i)$ of the wave function in the general form

$$\xi(k_{iT};\lambda) = \sum_p \bar{u}(k_{T1},\lambda_1)\Gamma_p v(k_{T2},\lambda_2), \tag{2.10}$$

with the Lorentz 4×4 matrices Γ_p represented by combinations of Dirac matrices and the constituent momenta, k_i. Using the Dirac equations for the free u and v spinors it is easily shown that the sum in Eq. (2.10) reduces to two terms involving either γ_5 or $[\not{k}_1,\not{k}_2]\gamma_5$. The most general wave function Ψ^α for a pseudoscalar meson can thus be written in the form

$$\Psi^\alpha(k_{iT};\lambda;\tau_i) = \chi^\alpha_{\tau_1\tau_2}\sqrt{2}\frac{\sqrt{m_1 m_2}}{\sqrt{\mathcal{M}^2-(m_1-m_2)^2}}\bar{u}(k_{T1},\lambda_1)\left\{\gamma_5\Phi_P(\mathcal{M}) + [\not{k}_1,\not{k}_2]\gamma_5\Phi_T(\mathcal{M})\right\}v(k_{T2},\lambda_2). \tag{2.11}$$

We shall assume that the two spin independent wave functions appearing in Eq. (2.11) can be parametrized with a Gaussian shape of Eq. (2.9) having the same momentum size parameter β:

$$\Phi_P(\mathcal{M}) = \Phi(\mathcal{M})\ , \Phi_T(\mathcal{M}) = r_{PT}\frac{1}{\mathcal{M}\beta}\Phi(\mathcal{M}). \tag{2.12}$$

Since the tensor term in Eq. (2.11) explicitly involves higher powers of the constituent longitudinal and transverse variables whose ranges are related to $\mathcal{M}$ and β, respectively, we have chosen the $\mathcal{M}\beta$ factor as the relative normalization between the Φ_P and Φ_T terms in Eq. (2.12). The dimensionless, numerical coeficient r_{PT} will then be determined by fitting various properties of the pion. In the $r_{PT}=0$ limit the wave function of Eq. (2.11) reduces to the one of Eq. (2.7) and corresponds to the $S=L=0$ state in the meson rest frame. The tensor term introduces an $L=1$ orbital component which mixes the $S=L=1$ lower with $S=L=0$ upper components of the Dirac spinors to give an overall $J^P=0^-$ state.

III. NUMERICAL RESULTS

A. π electromagnetic form factor

Before detailing the quark distributions given by the generalized wave functions including the additional tensor component Φ_T we shall present new results for the pion electromagnetic form factor. The form factor calculation for both noncovariant and covariant variable front models has been previously summarized [4]. For simplicity we maintain the same quark masses and oscillator size parameter β used in our previous calculations with $m_q=\beta=250$ MeV and vary r_{PT} to optimize the form factor description. It is significant to note that the tensor term drastically modifies the form factor behavior especially in the high momentum transfer region $Q^2>2$ GeV^2. Further as shown in Fig. 1 the generalized model provides an agreement with the data in this region without altering the correct low Q^2 behavior. As shown below the importance of the tensor term is further demonstrated in the analysis of the distribution amplitude and the structure functions.

B. Distribution amplitude

The quark distribution amplitude for a meson α, $\phi^\alpha(\xi)$, can in principle be obtained from the moments $\langle\xi^n\rangle$ [6],

$$\langle\xi^n\rangle = \int d\xi\xi^n\phi^\alpha(\xi) \tag{3.1}$$

which are formally defined by the matrix elements

$$\langle 0|\bar{\psi}(0)\gamma^\mu\gamma_5\frac{\lambda^\beta}{2}\overleftrightarrow{\partial}_{\mu_1}\cdots\overleftrightarrow{\partial}_{\mu_n}\psi(0)|P;\alpha\rangle$$

$$= if_\alpha\langle\xi^n\rangle\delta_{\alpha\beta}P^\mu P_{\mu_1}\cdots P_{\mu_n} + \text{trace}, \tag{3.2}$$

where the trace terms corresponding to higher twist operators have been omitted. Here f_α is the meson decay constant and the normalization is such that $\langle\xi^0\rangle=1$. The expansion of the quark field operators, $\psi,\bar{\psi}$ in terms of constituent $q\bar{q}$ creation and annihilation operators (see Eqs. (2.11) and (2.12)) leads to

$$\langle\xi^n\rangle = \frac{\sqrt{6}}{f_\alpha}\int\frac{d^3q_T}{(2\pi)^3}\frac{1}{\sqrt{M_\alpha}}\frac{m_1m_2}{\sqrt{k_{1L}k_{2L}\{\mathcal{M}^2-(m_1-m_2)^2\}}}\left(\frac{2q_T^3}{M_\alpha}+\frac{k_{1L}-k_{2L}}{M_\alpha}\right)^n\Phi(\mathcal{M})$$

$$\times\left[\frac{k_{1L}m_2+k_{2L}m_1}{m_1m_2} - r_{PT}\frac{2[(k_{1L}+k_{2L})^2-(m_1+m_2)^2]}{\beta(m_1+m_2)}\left(1-\frac{(m_1-m_2)(k_{1L}m_2-k_{2L}m_1)}{(k_{1L}+k_{2L})m_1m_2}\right)\right] \tag{3.3}$$

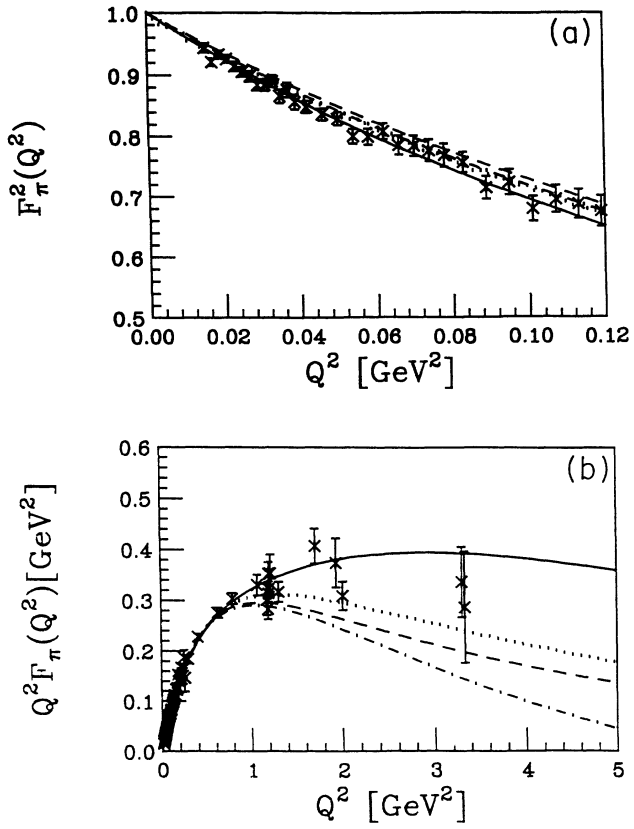

FIG. 1. Pion electromagnetic form factor. Solid line shows the result obtained with the $q\bar{q}$ wave function of Eq. (2.12) for $r_{PT} = 1.0$. Dashed line is the result of the covariant model of Ref. [4], dash-dotted and dotted lines are the results of relativistic models from Refs. [2,3], respectively. Data is taken from Ref. [21].

with $q_T = (q_T^3, q_T^\perp)$,

$$k_{iL} = \sqrt{m_i^2 + |q_T^2|},$$
$$\mathcal{M} = k_{1L} + k_{2L}, \tag{3.4}$$

and M_α being the meson mass. The decay constant f_α is calculated from Eq. (3.3) using $\langle \xi^0 \rangle = 1$ (see also Sec.V in Ref. [4]). In QCD, it can be shown that the physical part of the distribution amplitude $\phi^\alpha(\xi)$ is restricted for $-1 < \xi < 1$ [6] and for large n the moments in Eq. (3.2) behave as $\langle \xi^n \rangle \to 1/n^2$ implying that $\phi^\alpha(\xi \to \pm 1) \to 0$. In order to reproduce this feature in our model calculation we make the replacement

$$M_\alpha \to \mathcal{M} = k_{1L} + k_{2L} = \sqrt{m_1^2 + |q_T^2|} + \sqrt{m_2^2 + |q_T^2|}. \tag{3.5}$$

TABLE I. π and K mesons decay constant calculated with the formula of Eq. (3.3). The two set of results correspond to the use of spin averaged, constituent meson masses M and dynamical masses $\mathcal{M}$, respectively ($m_u = m_d = 250$ MeV, $m_s = 480$ MeV, $\beta = 250$ MeV, $r_{PT} = 1.0$)

	f_π[MeV]	f_K[MeV]
M	101	137
$\mathcal{M}$	75	104
Exp.	932	113

In Table I we list values for both π and K mesons decay constants calculated from Eq. (3.3) using spin averaged meson masses $M_\pi = 610$ MeV and $M_K = 790$ MeV and compare with results using dynamical masses for M_α determined by Eq. (3.5). Note that the experimental values lie almost midway between the two methods. The sensitivity to the mass prescription for normalized quantities such as moments of the distribution amplitude $\langle \xi^n \rangle$ or structure functions, which we analyze in the following subsection, is even smaller. Substituting Eq. (3.5) in Eq. (3.3) we make the following change of variables:

$$q_T^3 \to \xi(q_T) \equiv \frac{2q_T^3}{\mathcal{M}} + \frac{k_{1L} - k_{2L}}{\mathcal{M}}. \tag{3.6}$$

For fixed $q_T^\perp$ the variable $\xi(q_T)$ maps the domain of the variable q_T^3, $-\infty < q_T^3 < \infty$ into the finite interval $-1 < \xi(q_T) < 1$. The expression for the distribution amplitude can now be obtained from Eqs. (3.1), (3.3), (3.5), and (3.6) and is given by

$$\phi^\alpha(\xi) = \frac{\sqrt{6}}{f_\alpha} \int \frac{d^2q_T^\perp}{(2\pi)^3} \frac{1}{\sqrt{\mathcal{M}}} J(q_T^\perp, \xi) \frac{m_1 m_2}{\sqrt{k_{1L}k_{2L}\{\mathcal{M}^2 - (m_1 - m_2)^2\}}} \Phi(\mathcal{M})$$
$$\times \left[\frac{k_{1L}m_2 + k_{2L}m_1}{m_1 m_2} - r_{PT} \frac{2[(k_{1L} + k_{2L})^2 - (m_1 + m_2)^2]}{\beta(m_1 + m_2)} \left(1 - \frac{(m_1 - m_2)(k_{1L}m_2 - k_{2L}m_1)}{(k_{1L} + k_{2L})m_1 m_2} \right) \right] \tag{3.7}$$

with k_{iL} and $\mathcal{M}$, now functions of $q_T^\perp, \xi$, obtained from Eq. (3.4) using Eq. (3.6) to express $q_T^3 = q_T^3(\xi)$. $J(q_T^\perp, \xi)$ is the Jacobian of the transformation from $(q_T^3, q_T^\perp)$ to $(\xi, q_T^\perp)$. The explicit forms of the functions, $k_{iL}(q_T^\perp, \xi)$, $\mathcal{M}(q_T^\perp, \xi)$ and $J(q_T^\perp, \xi)$ are given in the Appendix.

In Figs. 2 and 3 we plot the function $\phi(\xi)$ for π and K mesons, respectively. In Fig. 2 the solid line gives our prediction for the set of parameters $m_q = \beta = 250$ MeV, $r_{PT} = 1.0$ which best describe the form factor shown in Fig. 1. The dashed line is the prediction for the pion distribution amplitude without the tensor term in the wave function of Eq. (2.11), i.e., with $r_{PT} = 0$. The wide, camel-like shape of the distribution amplitude obtained for $r_{PT} = 1.0$, a value that optimizes the form factor

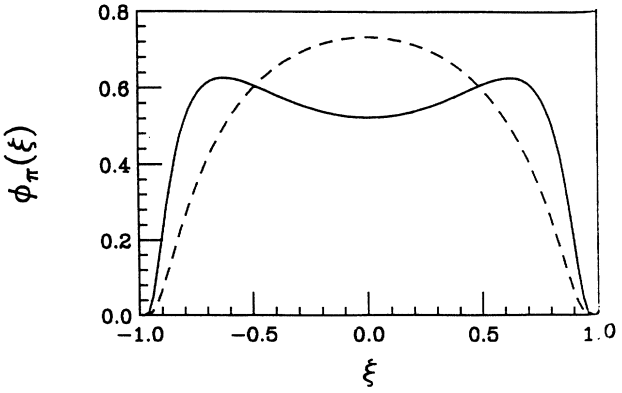

FIG. 2. Pion distribution amplitude with ($r_{PT} = 1$, solid curve) and without ($r_{PT} = 0$, dashed curve) the contribution from the tensor term in the $q\bar{q}$ wave function.

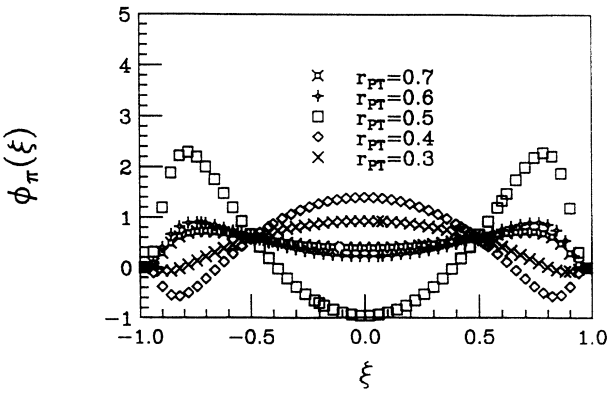

FIG. 4. r_{PT} dependence of the pion distribution amplitude.

description, is similar to that provided by the QCD sum rule approach [6] for the matrix element of Eq. (3.2), however, the predictions for the lowest moments $\langle\xi^2\rangle = 0.27$, $\langle\xi^4\rangle = 0.13$, are smaller than the ones of Chernyak and Zhitnitsky ($\langle\xi^2\rangle_{CZ} = 0.40$, $\langle\xi^4\rangle_{CZ} = 0.24$) yet closer to those obtained in Ref. [7] and lattice calculations [8,9]. The asymmetry in the K distribution amplitude in Fig. 3 is due to the large SU(3) breaking due to the strange quark mass ($m_s = 480$ MeV). Notice the sensitivity of the pion distribution amplitude to r_{PT} which is shown in Fig. 4. The largest sensitivity is observed for $r_{PT} \sim 0.5$ where the interference between the pseudoscalar and tensor terms is significant.

C. Structure functions

Structure functions contain important hadronic information and are obtained from inelastic processes. Accordingly we wish to further test our approach by computing the meson structure functions and comparing with available data usually extracted from Drell-Yan lepton [10,11] or charged hadron production [12] on nuclear targets using mesonic beams. The extraction of the structure functions from hadron production experiments is typically more complicated and somewhat model dependent due to uncertainties in the hadronization mechanism. In this paper the experimental pion structure function was extracted from the Drell-Yan muons produced by 252 GeV pions on tungsten [11]. The theoretical cross section for muon production as a function of longitudinal momentum fraction ξ_F of the muon pair is given by

$$\frac{d^2\sigma}{dQ^2 d\xi_F} = K\frac{4\pi\alpha^2}{9Q^4}\frac{[f_v^\pi(x_1)G_v^N(x_2) + f_s^\pi(x_1)G_s^N(x_2)]}{(\xi_F^2 + 4Q^2/s)^{1/2}},$$
$$x_{1,2} = [\pm\xi_F + (\xi_F^2 + 4Q^2/s)^{1/2}]/2, \tag{3.8}$$

where Q^2 and s are the mass of the muon pair and the square of the c.m. energy, respectively, and α is the electromagnetic fine structure constant. $f_{v(s)}^\pi(x_1)$ is the pion valence (sea) quark structure function and $G_{v(s)}^N(x_2)$ parametrizes the nuclear contribution. Assuming isospin symmetry for π^- we have

$$f_v^\pi(x) = x\bar{u}(x) = xd(x),$$
$$f_s^\pi(x) = xu_s(x) = x\bar{u}_s(x) = \cdots = x\bar{s}(x). \tag{3.9}$$

The nuclear contributions can be similarly parametrized in terms of valence and sea quark distributions of individual nucleons. The normalization (K factor) is measured to be $K \sim 1.75\pm0.13$ while a perturbative analysis to first order in α_s gives $K \sim 1.4$. The structure functions are in principle functions of x_i and Q^2, however, since we are describing the average data for $36.0 < Q^2 < 72.3$ GeV^2 we have suppressed the explicit Q^2 dependence. The meson structure functions can equivalently be defined in terms of a diagonal matrix element involving the commutator of two vector currents [16]

$$W_i^{\mu\nu}(x, Q^2) = \frac{1}{4\pi}\int dz e^{iqz}\langle p|[\bar{\psi}_i\gamma^\mu\psi_i(z), \bar{\psi}_i\gamma^\nu\psi_i(0)]|p\rangle \tag{3.10}$$

with $x = p\cdot q/M^2$, $Q^2 = -q^2 > 0$ and i referring to a particular flavor. Since it is known that the total longitudinal momentum of the hadron is only partially distributed among quarks, the constituent quarks which are assumed to carry the entire momentum of the hadron cannot be

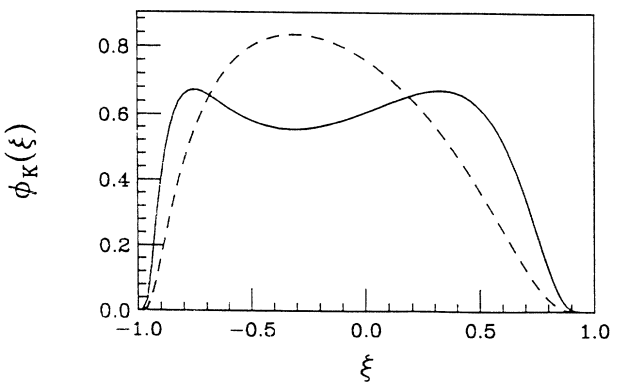

FIG. 3. Same as Fig. 2 for the K distribution amplitude.

identified with the partons contributing to deep inelastic structure functions. In the scaling limit, $Q^2 \to \infty$, Eq. (3.10) can be calculated using a short-distance expansion of the bilocal operator. In perturbative QCD scaling violations can be described in terms of a convolution of the partonic distributions defined at a scale of reference $Q_0^2 \ll \infty$ and the Altarelli-Parisi splitting functions which characterize the single parton response amplitudes for the change of scale due to radiation of gluons [17]. Here we also use the convolution approach [18] to relate our constituent quark model to the parton model. In a convolution model the quark distribution function for a hadron α, q_i^α, is represented by a product of the distribution function of a constituent quark, Q_v^α, in a hadron and the probability for a constituent quark to fragment into a QCD parton i, $q_{i/v}$,

$$q_i^\alpha(x,Q^2) = \int_x^1 \frac{dy}{y} Q_v^\alpha(x,Q_0^2) q_{i/v}\left(\frac{x}{y}, Q^2/Q_0^2\right). \quad (3.11)$$

The constituent quark distributions are defined through Eq. (3.10) with the QCD fields replaced by an effective constituent quark/gluon basis at $Q_0^2 \sim 1$ GeV^2. The Q^2 evolution of $q_{i/v}(x/y, Q^2/Q_0^2)$ is governed by perturbative QCD. However for any value of Q^2 phenomenological input is still required. For the average $Q^2 \sim 50$ GeV^2 of the Drell-Yan data the valence and sea quark distributions are

$$q_v^\pi(x) = \int_x^1 \frac{dy}{y} Q_v^\pi(x) q_{v/v}\left(\frac{x}{y}\right),$$
$$q_s^\pi(x) = \int_x^1 \frac{dy}{y} Q_v^\pi(x) q_{s/v}\left(\frac{x}{y}\right). \quad (3.12)$$

For the valence quark contributions in π^-, $q_v = q_d = q_{\bar{u}}$, while for the sea $q_s = q_d = q_{\bar{d}} = \cdots q_{\bar{s}}$. The number and momentum sum rules are, respectively,

$$\int_0^1 dx q_v^\pi(x) = 1,$$
$$2\int_0^1 dx x q_v^\pi(x) + 6\int_0^1 dx x q_s^\pi(x) = 1 - g_\pi, \quad (3.13)$$

where g_π represents the fraction of the gluon momentum in the pion currently measured as $g_\pi \sim 0.47$ [11]. The parton distributions in a constituent quark, $q_{i/v}$, are usually normalized to describe the relevant features of the low-x hadron scattering phenomenology. The Regge behavior at small x motivates the parametrization [18]

$$q_{v/v}(x) = \frac{\Gamma\left(A+\frac{1}{2}\right)}{\Gamma\left(\frac{1}{2}\right)\Gamma(A)} \frac{1}{\sqrt{x}} (1-x)^{A-1},$$
$$q_{s/v}(x) = \frac{C}{x}(1-x)^{D-1}, \quad (3.14)$$

with the parameters A, D, and C constrained by the momentum sum rule of Eq. (3.13):

$$\frac{1}{2A+1} + 6\frac{C}{D} = 1 - g_\pi.$$

Each can be determined by comparing the calculated quark distributions q_v^π and q_s^π to the data. The matrix element which determines the constituent quark distribution functions obtained from the light cone expansion of the current product in Eq. (3.10) has a very similar structure to Eq. (3.2) that defines the quark distribution amplitude. Using the techniques developed in the previous section the following expression for $Q_v^\alpha(x)$ is easily derived:

$$Q_v^\alpha(x) = \int \frac{d^2q_T^\perp}{(2\pi)^3} J(q_T^\perp, \xi) |\Phi(\mathcal{M})|^2 \times \left[1 + r_{PT}\frac{\mathcal{M}^2 - (m_1+m_2)^2}{\beta\mathcal{M}}\right]^2. \quad (3.15)$$

For $\alpha = \pi^-$, $m_1 = m_2$ the integrand is a symmetric function of $\xi = 2x-1$ yielding $Q_{\bar{u}}^{\pi^-}(x) = Q_d^{\pi^-}(x)$. For the kaon, $m_2 = m_s > m_1 = m_u = m_d$ and the nonstrange and strange quark distributions correspond to $\xi = 2x-1$ and $\xi = -2x+1$, respectively. Again $\mathcal{M} = \mathcal{M}(q_T^\perp, \xi)$ and $J(q_T^\perp, \xi)$ are specified in the Appendix.

In Fig. 5 we plot valence quark structure functions for the pion calculated in our model with $r_{PT} = 1.0$

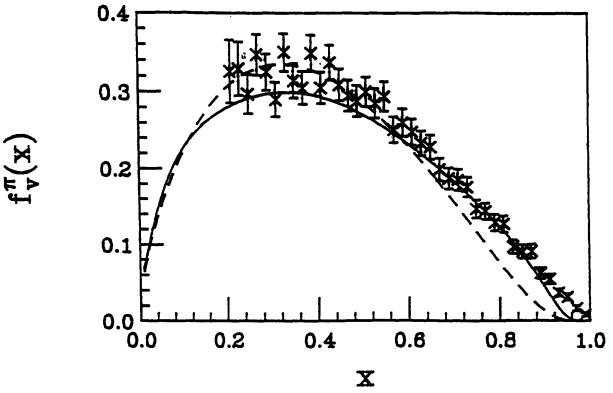

FIG. 5. Valence quark pion structure function $f_v^\pi(x) = xq_v(x)$ (curve convention same as in Fig. 2). Data is taken from Ref. [11].

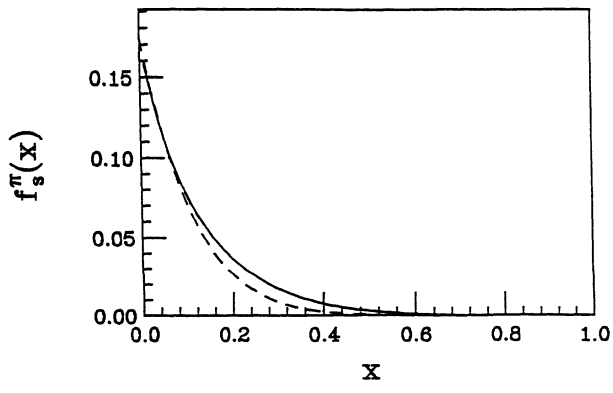

FIG. 6. Sea quark pion structure function. Solid line gives our model prediction with $r_{PT} = 1$, dashed line shows experimental parametrization, $f_s^\pi(x) = 0.173(1-x)^{8.4}$ of Ref. [11].

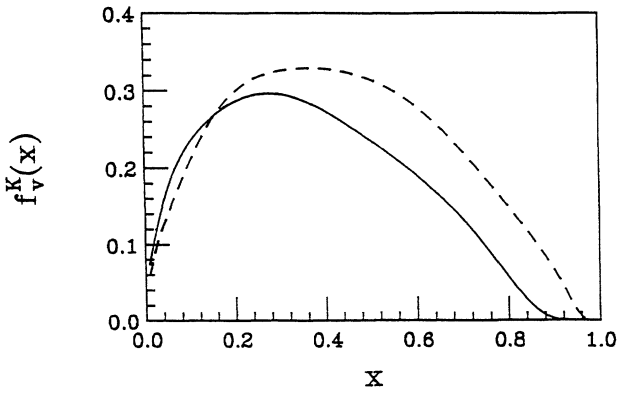

FIG. 7. Valence light quark (dashed line) and strange quark (solid line) kaon structure functions.

(solid line) obtained from the form factor fit and the result without the tensor component having $r_{PT} = 0$ (dashed line) and compare with data. The comparison suggests the importance of the tensor term at large x, $0.6 < x < 0.9$ where the sensitivity to the constituent quark distributions is the highest. In Fig. 6 we also compare our results for the sea quark distributions (solid line) with the curve used for experimental fitting (dashed line). The value $C = 0.086$ for the parameter in Eq. (3.14) is obtained by requiring the theoretical and experimental curves to agree at $x = 0$. Fitting A by the valence quark distribution yields $A = 0.75$ and the sum rule of Eq. (3.13) then gives $D = 4.0$. These numbers are in a good agreement with the ones obtained from the unpolarized nucleon structure function fits confirming hadron independence of the splitting functions $q_{i/v}(x)$ [18,19]. In Fig. 7 we also show our predictions for the strange (solid line) and light quark structure functions (dashed line) in kaon.

IV. SUMMARY AND CONCLUSIONS

Within the framework of our covariant variable front quark model, we have generalized the constituent, $q\bar{q}$ pion wave function and have studied the distribution amplitudes and structure functions. The meson observables analyzed in the paper, i.e., elastic form factors, decay constants, distribution amplitudes, and structure functions have been selected in the ordered of increasing complexity of the underlying matrix element. In principle all matrix elements involve QCD (partonic) fields and it is the mapping onto the effective (constituent) valence sector which, without a complete solution to the underlying dynamics, requires a model treatment. In our opinion we have implemented this mapping in a consistent way for all of the observables listed above. In the simplest case of the elastic form factors and decay constants matrix elements of local operators are involved so that no intermediate states appear and no explicit knowledge of the dynamics is required. In such a case we have directly approximated matrix elements of local QCD operators at $Q_0^2 \sim$ few GeV^2 hadronic scale by matrix elements of local effective operators evaluated in the impulse approximation in the valence quark hadronic basis. The moments of the soft distribution amplitudes that correspond to the leading twist operators can be treated in exactly the same manner since higher Fock space states do not explicitly contribute in this case. The situation is more complicated when considering deep inelastic structure functions, as one (i) begins with matrix element of a nonlocal operator, $W_{\mu\nu}$, and (ii) needs to extrapolate the matrix elements to a scale of large momentum transfer $Q^2 \sim 50$ GeV^2. Despite the fact that in the high-Q^2 limit operator product expansion (OPE) can be used to express the structure functions in terms of matrix elements of local operators the latter cannot be evaluated from the valence wave function alone due to a large momentum scale mismatch. A possible solution to this problem is provided by the convolution model which has been used in Sec. III. In the convolution model the matrix elements of QCD operators at large momentum scale in the impulse approximation receive contributions from hadronic wave functions describing low momentum valence constituents at Q_0^2 and from the constituent quark structure through QCD evolution to large momentum Q^2. The convolution model and factorization approach both respect the basic assumptions of our mapping from QCD to constituent quarks which have been summarized above. Furthermore in the convolution model the sensitivity of the calculated structure functions to details of the constituent quark structure and to the constituent valence wave function are well separated between small and large x, respectively. Thus even with the necessity of the constituent quark structure functions we were still able to test the hadronic valence wave function by going to the large-x region.

The extended model provides excellent agreement with the experimental data for the structure functions and the electromagnetic form factor as well as a good description of the decay constants. The improved description is due to a tensor component in the wave function which is a relativistic correction in the rest frame. We have also computed the structure functions and the distribution amplitudes with the wave function of Eq. (2.11) in a light cone quantization scheme and find results are similar to the variable front model. The results will be presented elsewhere. This confirms front independence of our results and is consistent with a previous assertion [4] that different front formulations do not lead to significant differences in the predictions for various mesonic properties. The magnitude of the tensor term which optimizes both the form factor and structure function now indicates a camel shape distribution amplitude with the dip at $\xi = 0$ although not as profound as the one suggested by early QCD sum rule calculations, but quite similar to recent nonlocal QCD sum rule calculations and lattice results. Since the shape and the moments of the quark distribution amplitude are very sensitive to the interference between the pseudoscalar and tensor components of the wave function the detailed knowledge of the former will provide important information on the structure of the meson wave function. As mentioned in the Introduction, the distribution amplitude is not directly mea-

surable, however, information on the magnitude of the lowest moments can be extracted from the meson form factor describing the hadronic part of the e meson $\to e\gamma$ transitions [6,20]. Finally, distribution amplitude studies provide an effective forum for theoretical comparisons of alternative model formulations which can provide significant insight into QCD dynamics.

ACKNOWLEDGMENTS

Financial support from U.S. D.O.E. Grants Nos. DE-FG05-88ER40461 and DE-FG05-90ER40589 is acknowledged.

APPENDIX

The variable change of Eq. (3.6) gives

$$q_T^3(q_T^\perp,\xi)=\frac{\mu_1^2(q_T^\perp)(1-\xi)^2-\mu_2^2(q_T^\perp)(1+\xi)^2}{\sqrt{8(1-\xi^2)[\mu_1^2(q_T^\perp)(1-\xi)+\mu_2^2(q_T^\perp)(1+\xi)]}},$$

where

$$\mu_i^2(q_T^\perp)\equiv m_i^2+(q_T^\perp)^2,$$

$$k_{iL}(q_T^\perp,\xi)=\sqrt{\mu_i^2(q_T^\perp)+[q_T^3(q_T^\perp,\xi)]^2},$$

$$\mathcal{M}(q_T^\perp,\xi)=k_{1L}(q_T^\perp,\xi)+k_{2L}(q_T^\perp,\xi),$$

and the Jacobian $J(q_T^\perp,\xi)$ is given by

$$J(q_T^\perp,\xi)=2\frac{\xi}{1-\xi^2}[\overline{\mu}^2+(\Delta\mu)^2-2\xi\overline{\mu}\Delta\mu]-\frac{2}{1-\xi^2}\Delta\mu\overline{\mu}-2\xi\frac{\overline{\mu}^2(\Delta\mu)^2}{\overline{\mu}^2+(\Delta\mu)^2-2\xi\overline{\mu}\Delta\mu}+2(1-\xi^2)\frac{\overline{\mu}^3(\Delta\mu)^3}{\overline{\mu}^2+(\Delta\mu)^2-2\xi\overline{\mu}\Delta\mu},$$

with

$$\overline{\mu}=\overline{\mu}(q_T^\perp)\equiv\tfrac{1}{2}[\mu_1(q_T^\perp)+\mu_2(q_T^\perp)],\quad \Delta\mu=\Delta\mu(q_T^\perp)\equiv\tfrac{1}{2}[\mu_1(q_T^\perp)-\mu_2(q_T^\perp)].$$

[1] A. De Rújula, H. Georgi, and S.L. Glashow, Phys. Rev. D **12**, 147 (1975); O. W. Greenberg, Annu. Rev. of Nucl. Part. Phys. **28**, 327 (1978); D.P. Stanley and D. Robson, Phys. Rev. D **21**, 3180 (1980); S. Godfrey and N. Isgur, *ibid.* **32**, 189 (1985); S. Capstick and N. Isgur, *ibid.* **34**, 2809 (1986).

[2] Z. Dziembowski and L. Mankiewicz, Phys. Rev. Lett. **55**, 2175 (1987); Z. Dziembowski, Phys. Rev. D **37**, 2030 (1988); **37**, 778 (1988); C.-R. Ji and S.R. Cotanch, *ibid.* **41**, 2319 (1990); C.-R. Ji, P.L. Chung, and S.R. Cotanch, *ibid.* **45**, 4214 (1992).

[3] F. Coester, in *Nuclear and Particle Physics on the Light Cone*, Proceedings of the Workshop, Los Alamos, New Mexico, 1988, edited by M. Johnson and L. Kisslinger (World Scientific, Singapore, 1989); P.L. Chung, F. Coester, and W. N. Polyzu, Phys. Lett. B **205**, 545 (1988); P.L. Chung and F. Coester, Phys. Rev. D **44**, 229 (1991).

[4] A. Szczepaniak, Chueng-Ryong Ji, and S.R. Cotanch (unpublished).

[5] G.R. Farrar and D.R. Jackson, Phys. Rev. Lett. **43**, 246 (1979); G.P. Lepage and S.J. Brodsky, Phys. Rev. D **22**, 2157 (1980); N. Isgur and C.H. Llewellyn Smith, Phys. Rev. Lett. **52**, 1080 (1984); Nucl. Phys. **B317**, 526 (1989); A. Szczepaniak and A.G. Williams, Phys. Lett. B **302**, 97 (1993).

[6] V.L. Chernyak and I.R. Zhitnitsky, Phys. Rep. **112**, 173 (1984).

[7] S.V. Mikhalov and A.V. Radyushkin, Yad. Fiz. **49**, 754 (1989) [Sov. J. Nucl. Phys. **49**, 494 (1989)].

[8] S. Gottlieb and A.S. Kronfeld, Phys. Lett. **55**, 2531 (1985); G. Martinelli and C.T. Sachrajda, Phys. Lett. B **190**, 151 (1987); **196**, 184 (1987); **217**, 319 (1989).

[9] D. Daniel, R. Gupta, and D.G. Richards, Phys. Rev. D **43**, 3715 (1991).

[10] R. Barate *et al.*, Phys. Rev. Lett. **43**, 1541 (1979).

[11] J.S. Conway *et al.*, Phys. Rev. D **39**, 39 (1989).

[12] A.V. Batunin *et al.*, Yad. Phys. **42**, 424 (1985) [Sov. J. Nucl. Phys. **42**, 268 (1985)]; M. Adamus *et al.*, Z. Phys. C **39**, 301 (1988); 311 (1988).

[13] P.A.M. Dirac, Rev. Mod. Phys. **21**, 392 (1949); H. Leutwyler and J. Stern, Ann. Phys. (N.Y.) **112**, 94 (1978); F. Coester and W.N. Polyzou, Phys. Rev. D **26**, 1348 (1982).

[14] S.J. Brodsky, T. Huang, and G.P. Lepage, in *Quarks and Nuclear Forces*, edited by D. Fries and B. Zeitnitz (Springer Tracts on Modern Physics, Vol. 100) (Springer-Verlag, NY, 1982); C.-R. Ji and Y. Surya, Phys. Rev. D **46**, 3565 (1992).

[15] N. Isgur, Acta Phys. Pol. B **8**, 1081 (1977); Z. Dziembowski, Phys. Rev. D **37**, 768 (1988).

[16] C. Itzykson and J.-B. Zuber, *Quantum Field Theory* (McGraw-Hill, NY, 1989).

[17] F.J. Ynduráin, *Quantum Chromodynamics* (Springer-Verlag, NY, 1983).

[18] G. Altarelli, N. Cabibbo, L. Maiani, and R. Petronzio, Nucl. Phys. **B69**, 531 (1974); Phys. Lett. **48B**, 435 (1974).

[19] Z. Dziembowski, H.J. Weber, L. Mankiewicz, and A. Szczepaniak, Phys. Rev. D **39**, 3257 (1989).

[20] A. Szczepaniak and A.G. Williams (unpublished).

[21] J. Bebek *et al.*, Phys. Rev. D **17**, 1693 (1978), S.R. Amendolia *et al.*, Nucl. Phys. **B277**, 168 (1986).